

Synthesis of new high molecular weight phosphorylated chitosans for improving corrosion protection

Clément Coquery, Claire Negrell, Nicolas Caussé, Nadine Pébère, Ghislain David

▶ **To cite this version:**

Clément Coquery, Claire Negrell, Nicolas Caussé, Nadine Pébère, Ghislain David. Synthesis of new high molecular weight phosphorylated chitosans for improving corrosion protection. Pure and Applied Chemistry, 2019, 17th International Conference on Polymers and Organic Chemistry (POC-17), 91 (3), pp.509-521. 10.1515/pac-2018-0509 . hal-02067816

HAL Id: hal-02067816
https://hal.science/hal-02067816

Submitted on 6 Nov 2019

HAL is a multi-disciplinary open access archive for the deposit and dissemination of scientific research documents, whether they are published or not. The documents may come from teaching and research institutions in France or abroad, or from public or private research centers.

L'archive ouverte pluridisciplinaire **HAL**, est destinée au dépôt et à la diffusion de documents scientifiques de niveau recherche, publiés ou non, émanant des établissements d'enseignement et de recherche français ou étrangers, des laboratoires publics ou privés.

OATAO
Open Archive Toulouse Archive Ouverte

Open Archive Toulouse Archive Ouverte (OATAO)

OATAO is an open access repository that collects the work of Toulouse researchers and makes it freely available over the web where possible

This is an author's version published in: http://oatao.univ-toulouse.fr/24659

Official URL: https://doi.org/10.1515/pac-2018-0509

To cite this version:

Coquery, Clément and Negrell, Claire and Caussé, Nicolas and Pébère, Nadine and David, Ghislain *Synthesis of new high molecular weight phosphorylated chitosans for improving corrosion protection.* (2019) In: 17th Polymers and Organic Chemistry (POC-2018), 4 June 2018 - 7 June 2018 (Palavas les Flots,, France).

Any correspondence concerning this service should be sent to the repository administrator: tech-oatao@listes-diff.inp-toulouse.fr

Conference paper

Clément Coquery, Claire Negrell, Nicolas Caussé, Nadine Pébère and Ghislain David*

Synthesis of new high molecular weight phosphorylated chitosans for improving corrosion protection

https://doi.org/10.1515/pac-2018-0509

Abstract: Two grades of chitosan [chitosan 30 000 g mol^{-1} (N-chitosan 30) and 250 000 g mol^{-1} (N-chitosan 250)] were functionalized by the Kabachnik–Fields reaction. To obtain the highest phosphonic ester grafting rate (55 % and 40 % for the N-chitosan 30 and N-chitosan 250, respectively), the pH must be kept constant during the reaction (pH = 5). Then, a partial hydrolysis of the ester functions was carried out in HCl medium to generate phosphonic acid functions up to 25 % and 20 % for the N-chitosan 30 and N-chitosan 250, respectively. It was shown that the grafting of phosphonic acids on chitosan significantly reduced the dynamic viscosity. Afterwards, electrochemical impedance measurements were performed in an aqueous solution (pH = 5) in the presence of either N-chitosans or P-chitosans (3 wt.%). The two native N-chitosans were little adsorbed onto the carbon steel surface and the corrosion protection was low. In contrast, the impedance results in the presence of the 30 000 g mol^{-1} phosphorylated chitosan (P-chitosan 30) evidenced the beneficial effect of grafted phosphonic acid on its adsorption on the steel surface. The lower efficiency of the 250 000 g mol^{-1} (P-chitosan 250) was attributed to its high molecular weight which made difficult the interactions between the phosphonic groups and the metallic surface.

Keywords: electrochemical impedance spectroscopy; grafting; Kabachnik–Fields reaction; phosphonic acid; POC-2018; polymer adsorption.

Introduction

Chitosan is a linear copolymer of glucosamine and N-acetyl-glucosamine, obtained from chitin by alkaline deacetylation [1] or from enzymatic pathway [2]. Chitosan is the second most abundant bio-based polysaccharide in the world after cellulose and is the major component in crustaceans, exoskeletons, fungi or insects [3]. Chitosan exhibits interesting properties: it is biocompatible [4], non-toxic [5], anti-bacterial [6] and allows film forming [7, 8]. Interest in chitosan materials is quite recent compared to cellulose. Therefore, chitosan

Article note: A collection of papers presented at the 17th Polymers and Organic Chemistry (POC-2018) conference held 4–7 June 2018 in the congress center, Palavas les Flots, France.

***Corresponding author: Ghislain David,** Institut Charles Gerhardt (ICG), UMR-5253, CNRS, UM, ENSCM, Ingénierie et Architectures Macromoléculaires (IAM), 240 avenue Emile Jeanbrau, 34296 Montpellier Cedex 5, France, e-mail: ghislain.david@enscm.fr
Clément Coquery: Institut Charles Gerhardt (ICG), UMR-5253, CNRS, UM, ENSCM, Ingénierie et Architectures Macromoléculaires (IAM), 240 avenue Emile Jeanbrau, 34296 Montpellier Cedex 5, France; and CIRIMAT, Université de Toulouse, CNRS, ENSIACET, 4 allée Emile Monso, CS 44362, 31030 Toulouse, France
Claire Negrell: Institut Charles Gerhardt (ICG), UMR-5253, CNRS, UM, ENSCM, Ingénierie et Architectures Macromoléculaires (IAM), 240 avenue Emile Jeanbrau, 34296 Montpellier Cedex 5, France
Nicolas Caussé and Nadine Pébère: CIRIMAT, Université de Toulouse, CNRS, ENSIACET, 4 allée Emile Monso, CS 44362, 31030 Toulouse, France

This work is licensed under a Creative Commons Attribution-NonCommercial-NoDerivatives 4.0 International License. For more information, please visit: http://creativecom

is one of the most promising materials derived from renewable resources and is currently explored very intensively [9]. Unmodified chitosan has been widely used in a variety of applications: for example as wound dressing [10], in tissue engineering [11], cosmetics [12], food [13] or textile industry [14], and in waste water treatment [15]. Specific functions can also be introduced to achieve original chitosan derivatives with new physicochemical properties and improved performances for selected applications.

The protection of metallic materials against corrosion with environmentally friendly compounds is an important aspect due to new strict environmental regulations. It is well-known that organic compounds which contain oxygen, nitrogen or sulfur groups can be adsorbed onto metallic surface and block the active corrosion sites [16–19]. Recently, some studies focused on the use of renewable resources, such as pectins, cellulose derivatives, alginates starch, chitin and chitosan due to their low toxicity and biodegradability [20, 21]. Chitosan has already been used as polymeric corrosion inhibitor on steel [22] and on copper [23] substrates, mainly in acidic conditions. Size of macromolecules could be an advantage by comparison with the corresponding monomers. Moreover, a large number of functionalization can be considered to enhance anchoring or adsorption on metallic surfaces. For instance, carboxymethyl chitosan [24, 25], O-fumaryl-chitosan [26], β-cyclodextrin modified chitosan [27], N-(2-hydroxy-3-trimethyl ammonium)propyl chitosan chloride [28], polyamine grafted chitosan copolymer [29], 2-N,N-diethylbenzene ammonium chloride N-oxoethyl chitosan [30] and thiourea chitosan [31–34] were synthesized and used to inhibit corrosion of carbon steel in strongly acidic solutions. In most of these studies, the efficiency of native chitosan was not assessed. In consequence, the effect of the grafted functional groups onto chitosan was not demonstrated.

Phosphonic acid-containing polymers have numerous potential applications as they exhibit attractive properties in term of adhesion [35] and are of interest in corrosion inhibition [36, 37]. Furthermore, the phosphorous-containing molecules or polymers can act as adhesion promoters for different substrates such as aluminum, zinc and steel [38–40]. Several syntheses of phosphorous-containing chitosan derivatives have already been developed due to their interesting biological and physico-chemical properties. Currently, the most common chitosan phosphonation reaction is the Moedritzer reaction. Numerous papers reported on the introduction of N,N-methylenephosphonic acid groups onto chitosan using this reaction [41–44]. Some authors claimed a regioselective functionalization of the primary amines [44] and also an esterification reaction of the hydroxyl groups [45]. However, Lebouc et al. as well as Illy et al. noticed the predominance of the methylation of the amines leading to N-methyl and N,N-dimethyl chitosan based on the Leuckart–Wallart reaction [46, 47]. The synthesis of N-methylenephosphonic acid can be achieved in two steps. First, phosphonic ester groups were attached to the chitosan by the Kabachnik–Fields reaction and then, the phosphonic acid functions were recovered by a hydrolysis step. Illy et al. [46] performed this synthesis on oligo-chitosan (i.e. $M_n \approx 2\,500$ g mol^{-1}) with a maximum substitution degree of 45 %.

The aim of the present work was to demonstrate the feasibility to functionalize two chitosans of different molecular weight (i.e. 30 000 and 250 000 g mol^{-1}) by the Kabachnik–Fields reaction to obtain phosphonic acid groups after the hydrolysis of the N,N-methylene phosphonic ester group. The synthesized products were characterized by proton and phosphorus nuclear magnetic resonance spectroscopy (^{1}H NMR and ^{31}P NMR, respectively). Then, the second step was to evaluate the influence of the phosphonic acid grafting on the adsorption of the chitosans on a carbon steel surface. Viscosity and electrochemical measurements were performed in acidic medium at pH = 5. The behavior of the carbon steel/chitosan solution was characterized by electrochemical impedance spectroscopy as a function of exposure time.

Materials and methods

Materials

Chitosans of high molecular weight ($M_n \approx 250\,000$ g mol^{-1}, degree of deacetylation: 92 %, henceforth called N-chitosan 250) and of medium molecular weight ($M_n \approx 30\,000$ g mol^{-1}, degree of deacetylation: 92 %,

henceforth called N-chitosan 30) were purchased from Glentham Life Sciences society. Acetic acid (>99.7 %, Aldrich), formaldehyde (37 wt.% aqueous solution, Aldrich), diethyl ethylphosphonate (98 %, Aldrich), isopropanol (99 %, Aldrich), dimethyl phosphite (98 %, Aldrich), sodium acetate (>99 %, Aldrich), lithium bromide (99.9 %, Aldrich) and sodium azide (99.5 %, Aldrich) were used as received.

The metal substrate was a P275NL1 low carbon steel. Its composition (in wt.%) was: C = 0.16, Si = 0.4, Mn = 0.5–1.5, Cr = 0.3, Mn = 0.08, Ni = 0.5, Cu = 0.3 % and Fe to 100. The steel sample was machined to obtain a cylindrical rod of 1.13 cm in diameter (surface area = 1 cm^2). The lateral part of the rod was covered with a heat-shrinkable insulating sheath, leaving only the tip of the carbon steel in contact with the electrolyte. The electrode was wet ground with silicon carbide (SiC) papers down to grade 4000 and cleaned with ethanol.

In all the paper H1, H2, H3, H4, H5, and H6 refer to the protons in positions 1, 2, 3, 4, 5, and 6 of the glucosamine unit, respectively. H7 and H8 correspond to N**H**Ac and C$\mathbf{H_3}$ of NHAc, respectively. ^{1}H NMR (D_2O, 400 MHz, δ): 4.7–4.3 (m, H1); 4.1–3.3 (m, H3, H4, H5, H7); 3.2–2.8 (m, H2); 1.9 (s, H8).

Synthesis of N,N-methylene phosphonic ester chitosan

N,N-methylene phosphonic ester chitosan was synthesized by the Kabachnik–Fields reaction according to the protocol proposed by Illy et al. [46]. In a 250 mL three-neck round bottom flask, 1.0 g of chitosan [6.1 mmol of NH_2 groups, 1 NH_2 molar equivalent (eq.)] was dissolved at room temperature during 12 h in 99 g of a 0.5 wt.% acetic acid aqueous solution. After complete dissolution of chitosan, 0.75 g of a 37 wt.% formaldehyde solution (18.3 mmol, 3 eq) was added by dripping directly in the solution. The solution was stirred during 1 h and then the temperature was raised to 60 °C. Then, two methods were used:

(a) 5.80 g of dimethyl phosphite (48.8 mmol, 8 eq.) were added drop-wise with continuous stirring. The pH of the solution was measured every 30 min.
(b) 0.97 g of dimethyl phosphite (8.1 mmol, 1.3 eq.) were added drop-wise with continuous stirring every hour namely 5.8 g of dimethyl phosphite (48.8 mmol, 8 eq.) in the reaction entirely. The pH of the solution was kept constant to 5 by adding aliquots of NaOH.

The mixtures obtained from both methods were stirred at 60 °C for 7 h and a small portion of the mixture was sampled through a septum at different times and concentrated by freeze-drying for ^{1}H and ^{31}P NMR analysis. The polymer was recovered and purified by two precipitations in isopropanol.

^{1}H NMR (D_2O, 400 MHz, δ): 6.8 (s, ^{1}J 628 Hz, H11); 4.7–4.3 (m, H1, H1′); 4.1–3.3 (m, H3, H4, H5, H7); 3.8–3.7 (d, H10); 3.4 (d, H9, H12); 3.2–2.8 (m, H2); 2.5 (m, H2′); 1.9 (s, H8). ^{31}P NMR (D_2O, 161.9 MHz, δ): 31.5–30.5 (m, P1); 8.4 (m, $^1J_{31P,1H}$ 637 Hz, PA). IR (cm^{-1}): 3700–3000 (ν_{N-H}, ν_{O-H}); 2860 (ν_{C-H}); 1653 (amide I); 1592 (δ_{N-H} of RNH_2); 1540 (amide II); 1527 (δ_{N-H} of R_2NH); 780 ($\nu_{P=O}$); 1183–800 (ν_{C-O-C}, ν_{C-O}).

Hydrolysis of N,N-methylene phosphonic ester chitosan

N,N-methylene phosphonic ester chitosan previously synthesized was dissolved in water (1.0 g, 6.1 mmol) and the solution was stirred at 60 °C for 6 h. The hydrolysis of phosphonic ester to phosphonic acid was monitored by a decreased of the pH up to 1 with a solution of 37 wt.% of HCl. The products were precipitated twice in isopropanol, washed with isopropanol and finally dried under vacuum. The final products were identified by ^{1}H NMR and ^{31}P NMR.

^{1}H NMR (D_2O, 400 MHz, δ): 4.7–4.3 (m, H1, H1′, H1″); 4.1–3.3 (m, H3, H4, H5, H7); 3.8–3.7 (d, H10); 3.4 (d, H9); 3.2–2.8 (m, H2, H2″); 2.5 (m, H2′); 1.9 (s, H8). ^{31}P NMR (D_2O, 161.9 MHz, δ): 30.5–30.0 (m, P1); 21.1–22.0 (m, P2); 13.8–12.2 (m, P3); 12.2–10.2 (m, P4). IR (cm^{-1}): 3700–3000 (ν_{N-H}, ν_{O-H}); 2860 (ν_{C-H}); 1653 (amide I); 1592 (δ_{N-H} of RNH_2); 1540 (amide II); 1527 (δ_{N-H} of R_2NH); 780 ($\nu_{P=O}$); 1183–800 (ν_{C-O-C}, ν_{C-O}).

NMR spectroscopy

All ^{1}H and ^{31}P NMR measurements were performed in deuterium oxide (D_2O) using a Bruker Avance 400 MHz NMR spectrometer at a temperature of 25 °C. Shifts are given in ppm. All ^{31}P NMR measurements were achieved using a zg30 sequence with a relaxation time of 13 s and a 30 degree pulse to obtain quantitative information. Diffusion Ordered SpectroscopY (DOSY) experiments were performed using a 2D Stimulated Echo experiment using a pulse sequence stegp1s. The gradient strength was logarithmically incremented in 32 steps from 2 % up to 95 % of the maximum gradient strength. Diffusion times and gradient pulse durations were optimized for each experiment in order to achieve a 95 % decrease in the resonance intensity at the largest gradient amplitude. After Fourier transformation and baseline correction, the diffusion dimension of the 2D DOSY spectra was processed by the Bruker Top Spin software package. All experiments were acquired in D_2O at 25 °C.

Diethyl ethylphosphonate was used as an internal standard to determine the degree of substitution (DS) of phosphorylated chitosan after the hydrolysis step. The peak at 1 ppm in ^{1}H NMR, corresponding to $P(OC_2H_5)_2CH_2CH_3$ was calibrated for three protons and the peak at 38 ppm in ^{31}P NMR was calibrated for one phosphorus.

Gel permeation chromatography

Gel permeation chromatography (GPC) was achieved by a Varian PL-GPC50 with a refractive index (RI) as detector. Two aquagel-OH columns (8 µm), with a separation range between 200 and 200 000 g mol^{-1}, were used with an eluent flow of 1 mL min^{-1}. All molecular weight measurements were performed at 25 °C. The buffer used was prepared with 16.5 g of sodium acetate (1.6 wt.%), 30 g of acetic acid (2.9 wt.%), 1 g of lithium bromide and 0.2 g of sodium azide for 1 L of distilled water. Before injection, all chitosans were dissolved in the buffer and filtered with 0.20 µm porosity polyamide filters. The molecular weight was estimated by aqueous chromatography by using pullulan-equivalent standard method [48].

Dynamic viscosity measurements

Chitosan solutions for dynamic viscosity measurements were prepared by dissolving N-chitosans (0.5, 1, 2 and 3 wt.%) in 0.5 wt.% of acetic acid and P-chitosans were dissolved in deionized water. Then, the pH of each solution was adjusted to 5 by adding some drops of a NaOH solution (1 M). The dynamic viscosity was measured by an Advanced Rheometer AR1000. A cone and plate geometry was used for the measurements (cone angle: 0.0349 radian, radius: 60 mm, gap size: 50 µm). The shear rates ranged from 1 to 500 rpm with 5 points per log cycle. The experiments were conducted at 25 °C.

Electrochemical impedance spectroscopy

Electrochemical measurements were performed in a three-electrode cell. A platinum electrode and a saturated K_2SO_4 (E = 0.651 V/ENH) electrode were used as counter and reference electrodes, respectively. The rotating system was an Autolab RDE-2 rotating disk electrode. The carbon steel sample was used as working electrode with a rotation speed of 500 rpm. The bio-based polymers were dissolved in an aqueous solution (deionized water) at a concentration of 3 wt.% and the pH of the solution was adjusted to 5 (using either 1 M acetic acid or 1 M NaOH).

The working electrode was introduced in the aqueous solution. All electrochemical experiments were performed at room temperature (22 ± 3 °C). Electrochemical impedance measurements were carried out using a Biologic VSP apparatus. The impedance diagrams were obtained, for exposure times ranging from 1 h to

24 h, under potentiostatic conditions, at the corrosion potential, over a frequency range of 65 kHz to 10 mHz with 8 points per decade, using a 30 mV peak-to-peak sinusoidal voltage perturbation.

Results and discussion

The first part of the present work deals with the phosphorylation of the two grades of chitosan: high molecular weight ($M_n \approx 250\,000$ g mol^{-1}, N-chitosan 250) and medium molecular weight ($M_n \approx 30\,000$ g mol^{-1}, N-chitosan 30). After the functionalization via the Kabachnik–Fields reaction and the hydrolysis step, phosphorylated chitosan 250 000 g mol^{-1} and chitosan 30 000 g mol^{-1} are henceforth called P-chitosan 250 and P-chitosan 30, respectively. The second part evaluates the influence of the phosphonic acid grafting on the adsorption of the chitosan on a carbon steel surface.

Synthesis of N,N-methylene phosphonic acid chitosan

The Kabachnik–Fields reaction consists in a two-step reaction that allows phosphonic acid groups to be grafted onto chitosan (Fig. 1). First, dimethyl phosphite and formaldehyde are added in a solution of chitosan followed step by the hydrolysis of phosphonic ester groups to obtain the corresponding phosphonic acid.

To our knowledge, only two papers deal with the Kabachnik–Fields reaction onto chitosan. The first one, only evidenced the efficient phosphorylation by infrared spectroscopy [45] and the second one only focused on oligo-chitosan (2500 g mol^{-1}) was used, which is soluble in water in a large pH range [46, 49]. The authors synthesized phosphonic acids grafted onto chitosan at neutral pH for different experimental conditions with a maximum substitution degree of 45 % [46]. In the present work, chitosans of high molecular weights (N-chitosan 30 and N-chitosan 250) were used, which required an acidic medium to be solubilized. Phosphorylation reaction was first carried out onto N-chitosan 30, which was easier to handle and to solubilize compared to N-chitosan 250.

The degree of substitution (DS) of N,N-methylene phosphonic ester was assessed from ^{1}H NMR spectrum by comparing the peak intensities of the non-functionalized chitosan (>CH–NH_2) and the functionalized chitosan (>CH-NR_2) peaks. The DS of phosphorus grafting was quite low, around 10–15 %. Illy et al. obtained a higher degree of substitution of about 45 %, but the phosphorylation was performed on oligochitosan at neutral pH [46]. For the present work, a pH of 5 was required to solubilize the N-chitosan 30. To analyze the effect of the pH on the phosphorylation reaction, both the DS and the pH were followed as a function of the reaction time (Fig. 2a).

In Fig. 2a, it can be seen that when the reaction proceeds, the pH drastically decreases from 5 to 1. According to the literature, low pH values induced both degradation of the dimethyl phosphite and the formation of first phosphonic acid mono methyl ester and then phosphorous acid, thus explaining the low pH value [47, 50, 51]. Futhermore phosphorous acid does not allow efficient phosphorylation onto chitosan as already showed by Lebouc et al. [47]. As a consequence, the DS was low, below 10 %, even after 7 h. To overcome this problem, the pH of the solution was maintained at 5 by adding aliquots of NaOH 1 mol L^{-1}

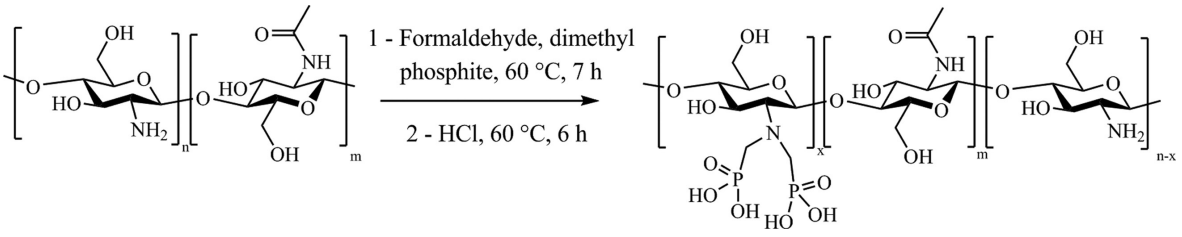


Fig. 1: Synthesis of N,N-methylene phosphonic ester chitosan followed by hydrolysis step.

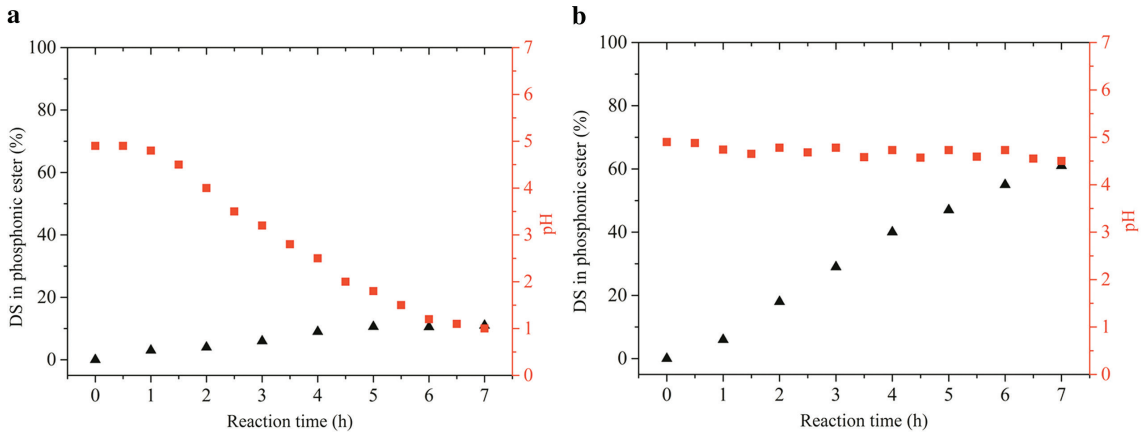


Fig. 2: DS of N,N-methylene phosphonic ester function on chitosan (black triangle) and pH during the reaction time (red square): (a) pH is free and (b) pH is maintained at 5 by adding NaOH.

every hour and dimethyl phosphite (1.3 eq: 1 eq NH_2) was also added throughout the reaction. Figure 2b shows the evolution of the N,N-methylene phosphonic ester groups DS onto chitosan for a constant pH value of 5. After 7 h, a DS close to 55 % is obtained. Thus, the negative effect of low pH on the chitosan phosphorylation reaction was suppressed. In order to verify if it is possible to obtain an even greater DS, the reaction is performed during 16 h and a DS of approximately 60 % was obtained, which seems to be a limit rate of functionalization of amines. Acidic hydrolysis of phosphonic ester groups has been widely used for the preparation of phosphonic acids [52]. In our case, the hydrolysis was also performed at pH 2 and 3, but no phosphonic acid moieties were obtained. A low pH equal to 1 was required for an efficient hydrolysis. The hydrolysis was performed during 6 h at 60 °C. P-chitosan 30 was recovered after at least three precipitations in isopropanol and dried during one night at 60 °C. Both ^{1}H NMR and ^{31}P NMR spectra of the N-chitosan 30 and the P-chitosan 30 before and after the hydrolysis step are showed in Figs. 3 and 4, respectively, and described below.

From the ^{1}H NMR spectrum of N-chitosan 30 (Fig. 3a) anomeric protons H1 are observed at high chemical shifts (4.3 ppm), due to their neighboring glycosidic and ring oxygen. H2 proton of glucosamine is observed at 3.1–3.2 ppm. The non-anomeric protons H3, H4, H5, H6 and H7 which are connected to ring-skeleton in a glycosyl residue, produce a broad signal in the middle of the spectrum due to their similar electron densities and, are observed between 3.5 and 4.0 ppm. Finally H8, observed at 2.0–2.1 ppm, represents three protons of N-acetyl glucosamine [53]. After the Kabachnik–Fields reaction onto N-chitosan 30, a shift (H2 at 3.1 ppm to H2′ at 2.5 ppm) of the proton located in the α position of the amine function of chitosan cycle is observed (Fig. 3b) [46]. Furthermore, a doublet is visible at 3.4 ppm (peak 8) and attributed to the methylene between phosphorus and nitrogen atoms. The results from ^{1}H NMR confirmed the synthesis of the phosphorylated chitosan. The ^{1}H NMR spectral analysis (Fig. 3c) does not give insight on its structure, apart from the signal intensity of protons situated in α position of the amine with N,N-methylene phosphonic acid (H2′) which is shifted to 3.1 ppm (H2″). The ^{1}H NMR allowed the functionalization of the chitosan through the Kabachnik–Fields reaction to be checked by the apparition of a new peak H2′. However, the overlap of peaks H2 and H2″ did not allow to confirm the efficient grafting of phosphonic acid. For this purpose, ^{31}P NMR was carried out to assess the efficient grafting of N,N-methylene phosphonic acid groups on P-chitosan 30.

For the P-chitosan 30 (Fig. 4a), a peak at 31 ppm (peak 1) is observed, corresponding to the N,N-methylene phosphonic ester groups: $R_2P(O)(OMe)_2$ [47, 54]. The small peak, around 28 ppm, may be attributed to dimethyl(hydroxymethyl)phosphonate which can be formed during the phosphorylation reaction. The presence of this compound reveals the effectiveness of the phosphorylation reaction onto chitosan and does not affect the next hydrolysis step. The disappearance of the peak around 14 ppm (^{1}J 723) [55] underlines the fact that dimethyl phosphite was almost fully removed after precipitation. A doublet of quadruplet is also observed at 6 and 10 ppm with a coupling constant of 674 Hz (peak A). This signal is attributed to mono

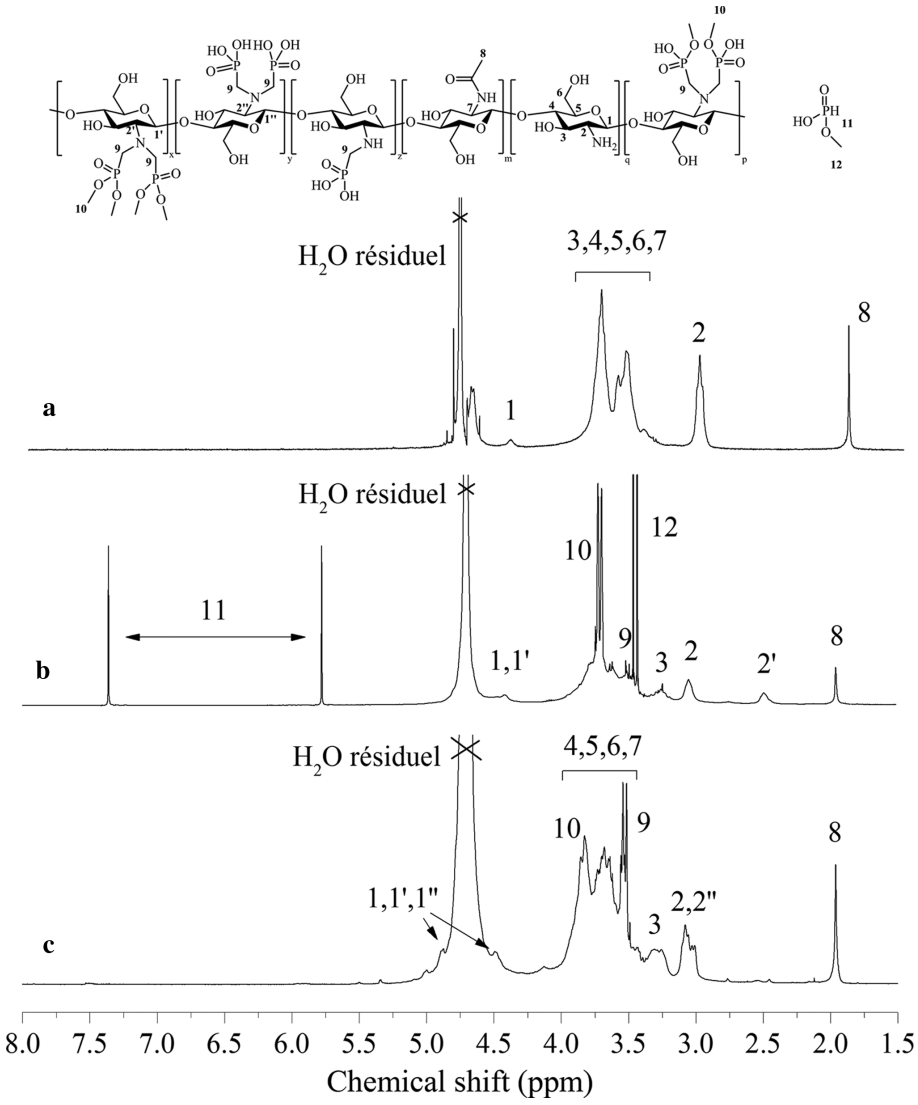


Fig. 3: ^{1}H NMR spectra recorded in D_2O at 25 °C of: (a) N-chitosan 30, (b) P-chitosan 30 and (c) P-chitosan 30 after the hydrolysis at pH = 1.

methyl phosphonic acid [46, 56]. Due to its strong interaction with the residual free amine of N-chitosan 30, mono methyl phosphonic acid was difficult to remove. However, it did not cause any problem for the hydrolysis reaction. A ^{31}P NMR spectrum of P-chitosan 30 after the hydrolysis step is shown in Fig. 4b. The initial peak at 31 ppm (peak 1) is partially shifted to 21 ppm (peak 2) corresponding to phosphonic monoester group and then is shifted to 11–13 ppm corresponding to phosphonic acid group (peaks 3 and 4) [46, 57]. The presence of two peaks at 11 and 13 ppm (respectively peaks 3 and 4) means that the two phosphorus groups are not equivalent. The peak 3 (13 ppm) probably corresponds to the function $N[(CH_2)P(O)(OH)_2]_2$ and the peak 4 (11 ppm) may be attributed to the $N(CH_2)P(O)(OH)_2$ function [56].

To confirm that the peaks 3 and 4 belong to the same molecule, DOSY ^{31}P NMR was carried out. DOSY NMR is a pseudo two-dimensional spectrum that displays chemical shifts along the horizontal axis and diffusion coefficients (D) along the vertical dimension [58]. It provides a way to distinguish peaks of chemical species spatially different and to separate compounds in a mixture based on their differing translation diffusion coefficients (D). The DOSY NMR can be considered as a chromatographic method for physical component separation and has been used to prove the chemical modification of chitosan with fumaric acid by

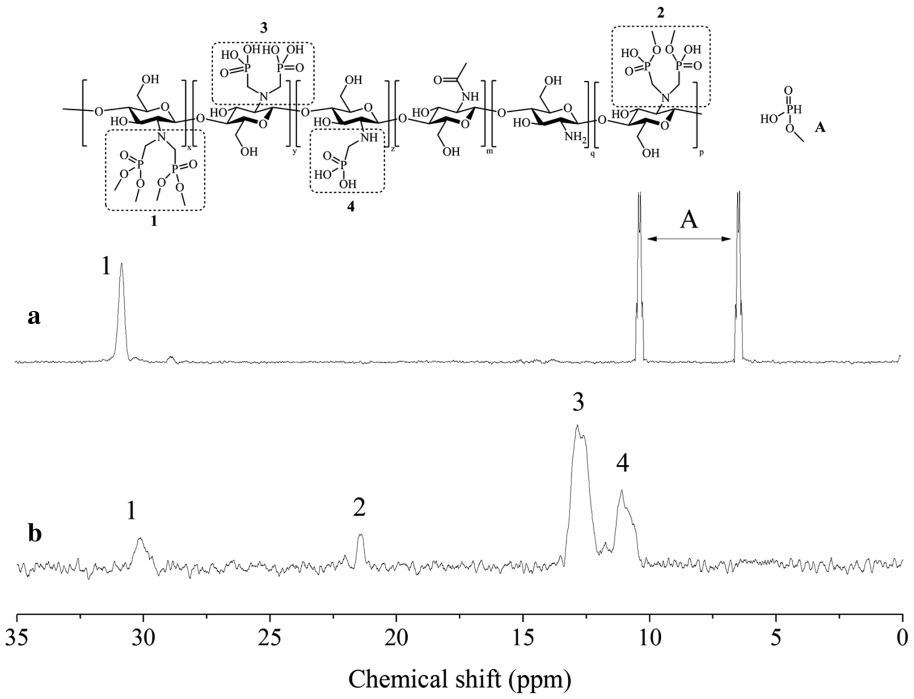


Fig. 4: ^{31}P NMR spectra recorded in D_2O at 25 °C of: (a) P-chitosan 30 and (b) P-chitosan 30 after the hydrolysis at pH = 1.

Wang and Liu [59]. Figure 5 shows the DOSY ^{31}P NMR spectrum of hydrolyzed P-chitosan 30; the different phosphorylated functions of the P-chitosan 30 provide four peaks (1, 2, 3 and 4) which are aligned along a horizontal line and have the same D value of 1.3×10^{-9} m^2 s^{-1}. Therefore, it can be definitively concluded that all the phosphorus-containing functions belong to the same chitosan molecule. To our knowledge, this is the first time that the DOSY ^{31}P NMR experiment was carried out on polymers to check the quality of the grafting.

Both ^{1}H and ^{31}P NMR analyses allowed evaluating a DS of about 25 % of phosphonic acid moieties for P-chitosan 30. This result is low since 55 % of primary amines were converted into N,N-methylene phosphonic ester groups, which can be ascribed to low N–C–P bond stability at pH = 1. The same procedure was applied onto N-chitosan 250. Table 1 summarizes the DS of phosphorylated functions obtained for the two chitosan grades via the Kabachnik–Fields reaction and after the hydrolysis step.

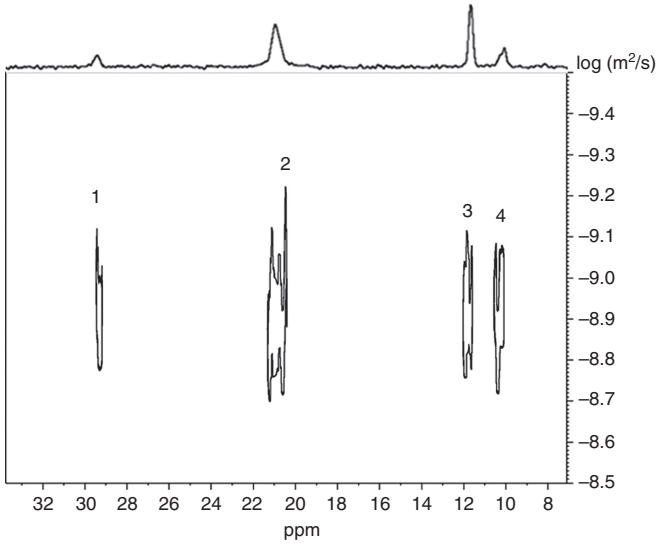


Fig. 5: ^{31}P DOSY NMR spectrum of P-chitosan 30 recorded in D_2O at 25 °C.

Table 1: DS (%)[a] and average molecular weight (M_w) for the two grades of chitosan via the Kabachnik–Fields reaction and after the hydrolysis step.

Samples	Before hydrolysis		After hydrolysis		
	N,N-methylene phosphonic ester	M_w (kg mol^{-1})	N,N-methylene phosphonic ester	N,N-methylene phosphonic mono ester	N,N- and N-methylene phosphonic acid	M_w (kg mol^{-1})
P-chitosan 30	55 %	35	5 %	5 %	25 %	32
P-chitosan 250	40 %	250	15 %	0 %	20 %	240

[a]Uncertainty of 5 % for each value given in the table.

From the data reported in Table 1, it can be seen that the higher the molecular weight the lower the DS. These results are probably linked to the chain length which limited the accessibility to the reactive functions. Noteworthy, M_w of P-chitosans was also estimated after phosphorylation and hydrolysis step from GPC and the same GPC traces were obtained, proving that both reaction steps do not affect the chitosan backbone.

Influence of the phosphonic acid grafting on the adsorption of the chitosan on a carbon steel surface

The dynamic viscosity of both the native and the phosphorylated chitosans was determined. The results are shown in Fig. 6. At low concentrations, it can be seen that the dynamic viscosity is almost identical for all the solutions. When the concentration increases, the viscosity of the chitosan increases due to the increase of polymer-polymer interactions.

The functionalization of the chitosan by the phosphonic acid groups decreases the dynamic viscosity of the solution. The viscosity of the N-chitosan 250 is reduced by a factor of 10 after phosphorylation with a DS around 20 % in phosphonic acid. Indeed, the phosphonic acids are known for their hydrophilic character [60, 61]. The same phenomenon is observed for the N-chitosan 30, where the viscosity is also reduced after phosphorylation.

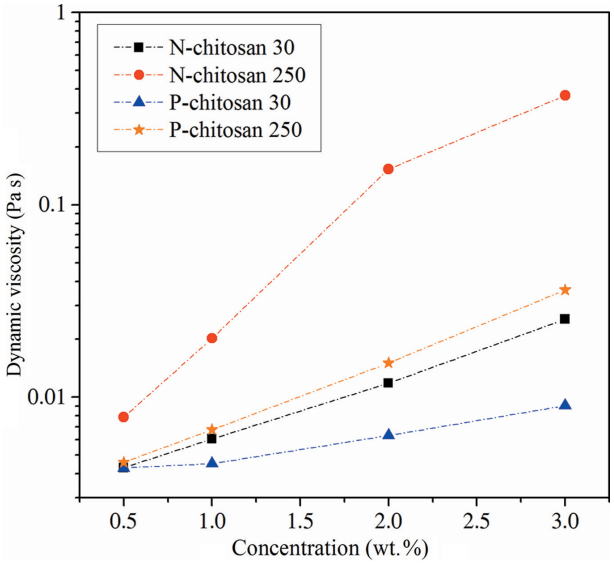


Fig. 6: Dynamic viscosity as a function of the chitosans concentration.

Electrochemical impedance measurements were achieved to investigate the effect of phosphorylation on the adsorption of the chitosan macromolecules on metallic surfaces in solution. The impedance diagrams were obtained consecutively for different immersion times (3 h, 6 h, 12 h and 24 h). The diagrams obtained with the N-chitosan 30 and the P-chitosan 30 are shown in Figs. 7 and 8, respectively. For the N-chitosan 30 (Fig. 7), the diagrams are little modified with the immersion time and they are almost superimposed. It can be noticed that they are strongly flattened (Nyquist representation) with a small phase angle (Bode representation). On the low frequency range, a well-defined inductive loop is observed, which is often attributed to the presence of adsorbed species on the electrode surface [62]. Even if the presence of the inductive loop revealed the presence of the N-chitosan 30 on the metal surface, the impedance values are low. For the P-chitosan 30 (Fig. 8), the diagrams are characterized by two capacitive loops and the size of the two loops increases when the immersion time increases. When the immersion time increases, a slight shift of the maximum frequency towards lower frequency can be noticed. The first time constant can be associated to the charge transfer process. After 24 h of immersion, the size of the first capacitive loop is about 10 times higher than that obtained with the N-chitosan 30. The second time constant is not well-defined and its characteristic frequency shifts towards lower frequencies when the immersion time increases and thus, after 24 h of immersion, only some points can be observed.

Similar impedance experiments were performed with N-chitosan 250 and P-chitosan 250. The diagrams (not shown) are similar to that obtained with the N-chitosan 30 or the P-chitosan 30. The impedance modulus at low frequency (10 mHz) was determined from the impedance spectra for the different systems (N-chitosans and P-chitosans) and for the different immersion times. The results are shown in Fig. 9. For the N-chitosan 30 and N-chitosan 250, the impedance values are relatively similar (about 100 Ω cm^2), independently of the immersion time. For the P-chitosan 30, the impedance values gradually increase from

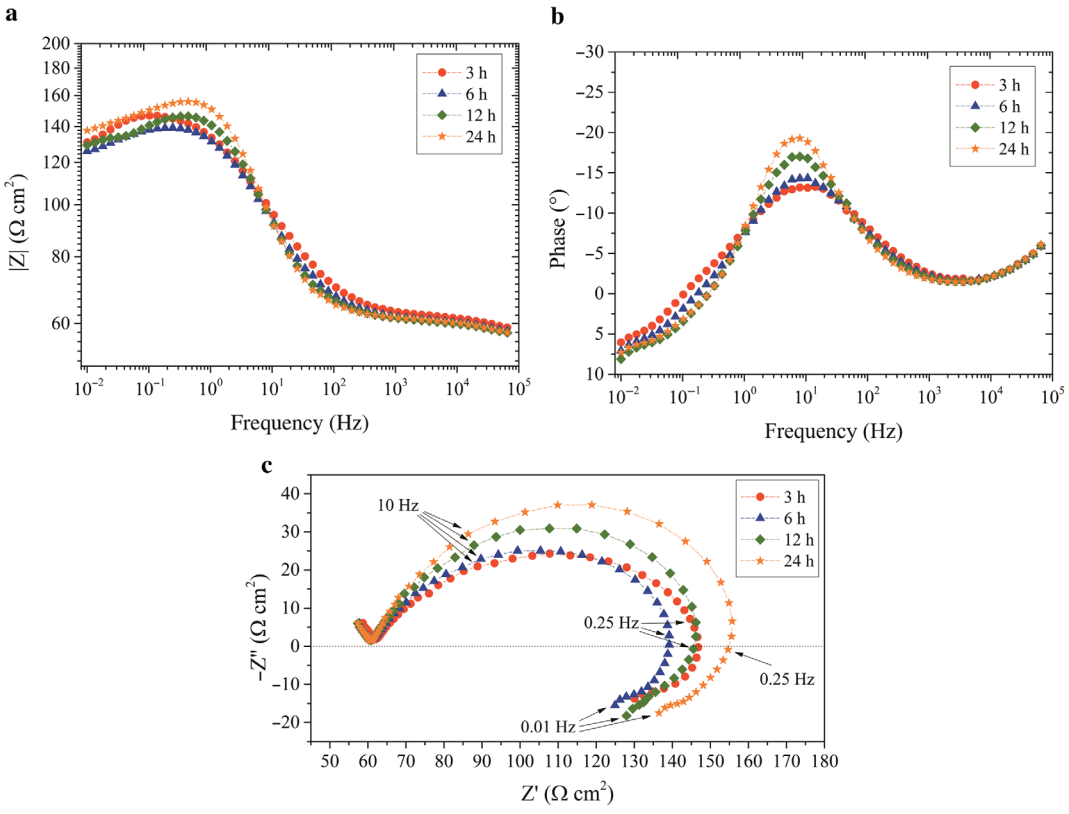


Fig. 7: Electrochemical impedance diagrams obtained for the carbon steel electrode after different immersion times in the aqueous solution at pH = 5 with 3 wt.% of N-chitosan 30: (a) Bode representation of the magnitude of the impedance, (b) Bode representation of the phase angle and (c) Nyquist representation.

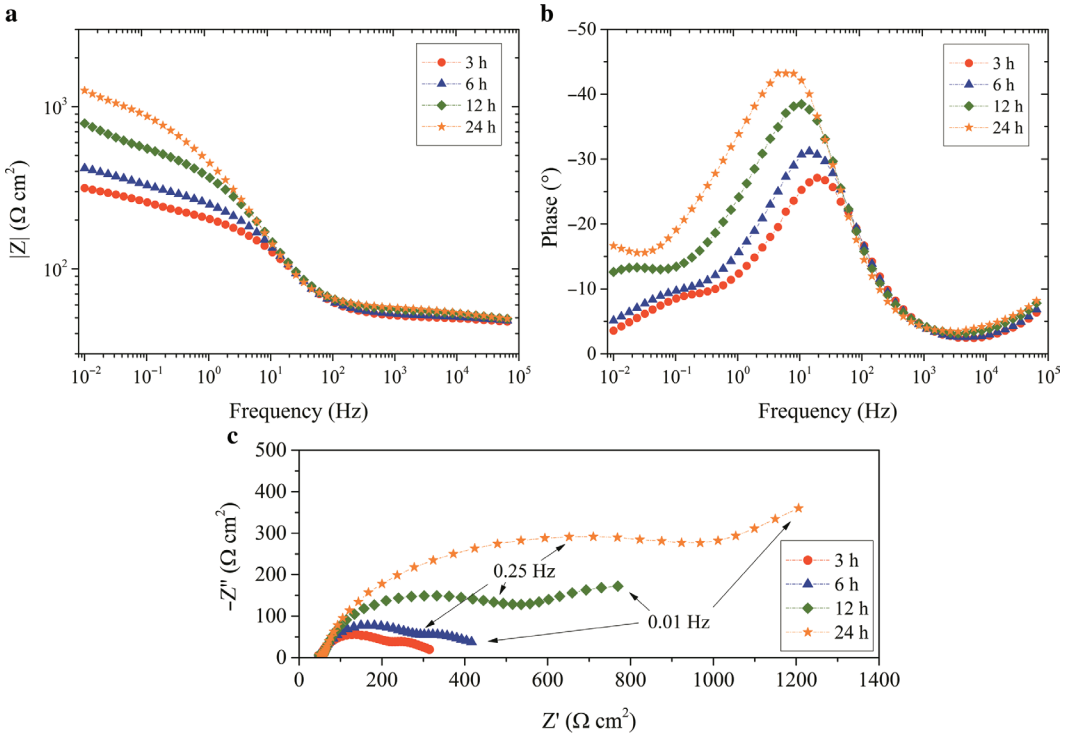


Fig. 8: As Fig. 7 for the P-chitosan 30.

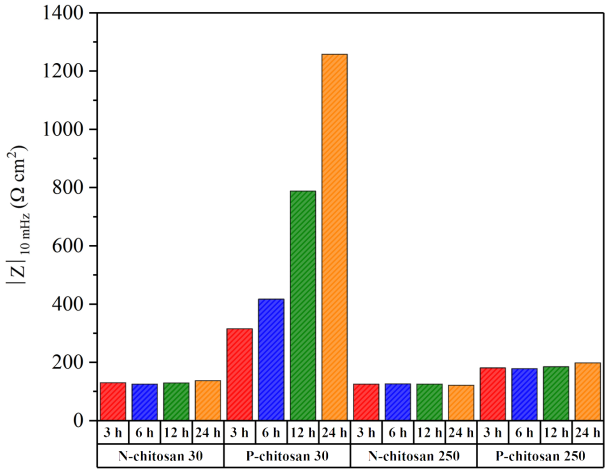


Fig. 9: Impedance modulus obtained at 10 mHz from the impedance diagrams for the carbon steel after different immersion times in the aqueous solution at pH = 5 with N-chitosans and P-chitosans.

3 h to 24 h. This would be indicative of higher interactions of the P-chitosan 30 with the metal surface, even if the two macromolecules exhibited comparable DS (Table 1). For the P-chitosan 250, the low impedance values can be attributed to the solution viscosity (Fig. 6) which limited the phosphonic groups to interact with the metal surface.

Chitosan naturally have amine and hydroxyl groups. These groups can interact with the steel surface via electrons of the oxygen and nitrogen atoms which can provide corrosion inhibition [22]. In the present work, it was shown that N-chitosans were adsorbed on the metal surface but slightly reduced the corrosion process, probably due to a weak anchorage and/or a low surface coverage. In contrast, the phosphonic acids grafted on the chitosan allowed a better adsorption of the bio-polymer to the metal surface.

Conclusions

This work was dedicated to the synthesis of phosphorylated chitosans for corrosion protection. First, the Kabachnik–Fields reaction was performed onto N-chitosans in acidic medium to obtain the N,N-and N-methylphosphonic ester. Acidic hydrolysis of the N,N- and N-methylphosphonic ester in the N,N- and N-methylphosphonic acid form allowed a grafting rate up to 25 % to be obtained. The functionalization was confirmed by ^{1}H NMR and ^{31}P NMR. Then, from electrochemical impedance measurements, it was shown that native chitosans was absorbed on the steel surface but they little decreased the corrosion rate. In contrast, the phosphonic acids grafted onto chitosan decreased the solution viscosity and increased the anchoring groups favoring the bio-polymer adsorption on the steel surface. However, in the case of the P-chitosan 250, the high molecular weight limited the accessibility of the phosphonic groups to the metallic surface.

Acknowledgment: This work is part of Clément Coquery PhD thesis, financially supported by the Direction Générale de l'Armement (DGA). The authors gratefully acknowledge the DGA for this support.

References

[1] S. K. Kim. *Chitin, Chitosan, Oligosaccharides and their Derivatives*, CRC Press, Boca Ratin (2011).
[2] I. Tsigos, A. Martinou, D. Kafetzopoulos, V. Bouriotis. *Trends Biotechnol.* **18**, 305 (2000).
[3] S.-K. Kim. *Chitin, Chitosan, Oligosaccharides and their Derivatives: Biological Activities and Applications*, 1st ed., CRC Press, Boca Raton (2010).
[4] P. J. VandeVord, H. W. T. Matthew, S. P. DeSilva, L. Mayton, B. Wu, P. H. Wooley. *J. Biomed. Mater. Res.* **59**, 585 (2002).
[5] M. Rinaudo. *Prog. Polym. Sci.* **31**, 603 (2006).
[6] S. Tokura, K. Ueno, S. Miyazaki, N. Nishi. Molecular weight dependent antimicrobial activity by chitosan, in *New Macromolecular Architecture and Functions*, P. M. Kamachi and P. A. Nakamura (Eds.), Springer, Berlin, Heidelberg, Vol. 21, pp. 199–207 (1996).
[7] P. K. Dutta, J. Dutta, V. S. Tripathi. *J. Sci. Ind. Res.* **63**, 20 (2004).
[8] J. Nunthanid, S. Puttipipatkhachorn, K. Yamamoto, G. E. Peck. *Drug Dev. Ind. Pharm.* **27**, 143 (2001).
[9] A. Gandini. *Macromolecules* **41**, 9491 (2008).
[10] G. Kratz, C. Arnander, J. Swedenborg, M. Back, C. Falk, I. Gouda, O. Larm. *Scand. J. Plast. Reconstr. Surg. Hand. Surg.* **31**, 119 (1997).
[11] M. Gingras, I. Paradis, F. Berthod. *Biomaterials* **24**, 1653 (2003).
[12] S.-K. Kim, Y. D. Ravichandran, S. B. Khan, Y. T. Kim. *Biotechnol. Bioproc. E* **13**, 511 (2008).
[13] H. K. No, S. P. Meyers, W. Prinyawiwatkul, Z. Xu. *J. Food Sci.* **72**, 87 (2007).
[14] S. Gowri, L. Almeida, T. Amorim, N. Carneiro, A. Pedro Souto, M. Fátima Esteves. *Text. Res. J.* **80**, 1290 (2010).
[15] I. G. Lalov, I. I. Guerginov, M. A. Krysteva, K. Fartsov. *Water Res.* **34**, 1503 (2000).
[16] G. L. Li, Z. Zheng, H. Möhwald, D. G. Shchukin. *ACS Nano* **7**, 2470 (2013).
[17] D. G. Shchukin, H. Möhwald. *Small* **3**, 926 (2007).
[18] D. Snihirova, S. V. Lamaka, M. F. Montemor. *Electrochim. Acta* **83**, 439 (2012).
[19] M. F. Montemor, D. V. Snihirova, M. G. Taryba, S. V. Lamaka, I. A. Kartsonakis, A. C. Balaskas, G. C. Kordas, J. Tedim, A. Kuznetsova, M. L. Zheludkevich, M. G. S. Ferreira. *Electrochim. Acta* **60**, 31 (2012).
[20] S. A. Umoren, U. M. Eduok. *Carbohydr. Polym.* **140**, 314 (2016).
[21] M. L. Zheludkevich, J. Tedim, C. S. R. Freire, S. C. M. Fernandes, S. Kallip, A. Lisenkov, A. Gandini, M. G. S. Ferreira. *J. Mater. Chem.* **21**, 4805 (2011).
[22] S. A. Umoren, M. J. Banera, T. Alonso-Garcia, C. A. Gervasi, M. V. Mirífico. *Cellulose* **20**, 2529 (2013).
[23] M. N. El-Haddad. *Int. J. Biol. Macromol.* **55**, 142 (2013).
[24] S. Cheng, S. Chen, T. Liu, X. Chang, Y. Yin. *Mater. Lett.* **61**, 3276 (2007).
[25] S. Cheng, S. Chen, T. Liu, X. Chang, Y. Yin. *Electrochim. Acta* **52**, 5932 (2007).
[26] Y. Sangeetha, S. Meenakshi, C. S. Sundaram. *Carbohydr. Polym.* **136**, 38 (2016).
[27] Y. Liu, C. Zou, X. Yan, R. Xiao, T. Wang, M. Li. *Ind. Eng. Chem. Res.* **54**, 5664 (2015).
[28] Y. Sangeetha, S. Meenakshi, C. Sairam Sundaram. *Int. J. Biol. Macromol.* **72**, 1244 (2015).
[29] H. Li, H. Li, Y. Liu, X. Huang. *J. Korean Chem. Soc.* **59**, 142 (2015).
[30] M. H. M. Hussein, M. F. El-Hady, H. A. H. Shehata, M. A. Hegazy, H. H. H. Hefni. *J. Surfactants Deterg.* **16**, 233 (2013).
[31] D. S. Chauhan, K. R. Ansari, A. A. Sorour, M. A. Quraishi, H. Lgaz, R. Salghi. *Int. J. Biol. Macromol.* **107**, 1747 (2018).

[32] A. M. Fekry, R. R. Mohamed. *Electrochim. Acta* **55**, 1933 (2010).
[33] M. Li, J. Xu, R. Li, D. Wang, T. Li, M. Yuan, J. Wang. *J. Colloid Interface Sci.* **417**, 131 (2014).
[34] M.-L. Li, R.-H. Li, J. Xu, X. Han, T.-Y. Yao, J. Wang. *J. Appl. Polym. Sci.* **131**, 40671 (2014).
[35] C. Brondino, B. Boutevin, J.-P. Parisi, J. Schrynemackers. *J. Appl. Polym. Sci.* **72**, 611 (1999).
[36] E. Kálmán, F. H. Kármán, J. Telegdi, B. Várhegyi, J. Balla, T. Kiss. *Corros. Sci.* **35**, 1477 (1993).
[37] X. H. To, N. Pebere, N. Pelaprat, B. Boutevin, Y. Hervaud. *Corros. Sci.* **39**, 1925 (1997).
[38] I. Felhősi, E. Kálmán. *Corros. Sci.* **47**, 695 (2005).
[39] I. Maege, E. Jaehne, A. Henke, H.-J. P. Adler, C. Bram, C. Jung, M. Stratmann. *Prog. Org. Coat.* **34**, 1 (1998).
[40] F. Millet, R. Auvergne, S. Caillol, G. David, A. Manseri, N. Pébère. *Prog. Org. Coat.* **77**, 285 (2014).
[41] D. R. Jayakumar, R. L. Reis, J. F. Mano. *J. Macromol. Sci. A* **44**, 271 (2007).
[42] V. M. Ramos, N. M. Rodríguez, M. F. Díaz, M. S. Rodríguez, A. Heras, E. Agulló. *Carbohydr. Polym.* **52**, 39 (2003).
[43] A. Zuñiga, A. Debbaudt, L. Albertengo, M. S. Rodríguez. *Carbohydr. Polym.* **79**, 475 (2010).
[44] A. Heras, N. M. Rodríguez, V. M. Ramos, E. Agulló. *Carbohydr. Polym.* **44**, 1 (2001).
[45] G. L. Matevosyan, Y. S. Yukha, P. M. Zavlin. *Russ. J. Gen. Chem.* **73**, 1725 (2003).
[46] N. Illy, G. Couture, R. Auvergne, S. Caillol, G. David, B. Boutevin. *RSC Adv.* **4**, 24042 (2014).
[47] F. Lebouc, I. Dez, P.-J. Madec. *Polymer* **46**, 319 (2005).
[48] J. M. Erdner, H. G. Barth, J. P. Foley, W. G. Payne. *J. Chromatogr. A* **1129**, 41 (2006).
[49] N. Illy, M. Robitzer, R. Auvergne, S. Caillol, G. David, B. Boutevin. *J. Polym. Sci. A: Polym. Chem.* **52**, 39 (2014).
[50] E. M. Georgiev, R. Tsevi, V. Vassileva, K. Troev, D. M. Roundhill. *Phosphorus Sulfur Silicon Relat. Elem.* **88**, 139 (1994).
[51] V. Vassileva, E. M. Georgiev, K. Troev, D. M. Roundhill. *Phosphorus Sulfur Silicon Relat. Elem.* **92**, 101 (1994).
[52] P. Jansa, O. Baszczyňski, E. Procházková, M. Dračínský, Z. Janeba. *Green Chem.* **14**, 2282 (2012).
[53] M. R. Kasaai. *Carbohydr. Polym.* **79**, 801 (2010).
[54] M. J. P. Harger, A. Williams. *J. Chem. Soc. Perkin Trans. 1* **0**, 1681 (1986).
[55] V. Mark, J. R. Van Wazer. *J. Org. Chem.* **32**, 1187 (1967).
[56] J. Tebby. *Handbook of Phosphorus-31 Nuclear Magnetic Resonance Data*, CRC Press, Boca Raton (1990).
[57] M. L. Rueppel, J. T. Marvel. *Org. Magn. Reson.* **8**, 19 (1976).
[58] Y. Cohen, L. Avram, L. Frish. *Angew. Chem. Int. Ed.* **44**, 520 (2005).
[59] K. Wang, Q. Liu. *Carbohydr. Res.* **386**, 48 (2014).
[60] C. Sevrain, H. Berchel, H. Couthon, P.-A. Joffrès. *Beilstein J. Org. Chem.* **13**, 2186 (2017).
[61] B. Rivas, E. Pereira, P. Galligos, D. Homper, K. Geckeler. *J. Appl. Polym. Sci.* **92**, 2917 (2004).
[62] H. H. Hassan, E. Abdelghani, M. A. Amin. *Electrochim. Acta* **52**, 6359 (2007).